

ISTITUTO NAZIONALE DI FISICA NUCLEARE

Sezione di Genova

INFN/FM-93/03
27 Luglio 1993

Bi Zhang, P.Fabbricatore, G.Gemme, R.Musenich, R.Parodi:

**STUDIES OF THE MECHANISM OF DISSIPATION AT RADIO
FREQUENCY IN HIGH TEMPERATURE SUPERCONDUCTING
MATERIALS**

**STUDIES OF THE MECHANISM OF DISSIPATION AT RADIO
FREQUENCY IN HIGH TEMPERATURE SUPERCONDUCTING
MATERIALS**

Bi Zhang, P.Fabbricatore, G.Gemme, R.Musenich, R.Parodi
INFN – Sezione di Genova, Via Dodecaneso 33, I-16146 Genova (Italia)

ABSTRACT

We report experimental results on the impedance of the high T_c superconducting material $YBa_2Cu_3O_7$ at radio frequency fields in various temperatures, rf magnetic fields and frequencies. A various kind of samples including polycrystalline pellets, thin films on $SrTiO_3$ and thick films on silver substrates have been measured in this work. A host cylindrical silver cavity, operated at its TE₀₁₁ mode at 7.9 GHz, was utilised in the radio frequency measurements for small samples. These samples were inserted or just replace the end-plates of the host cavity to form a sample-cavity mixed system. The sensibility and limit of the host cavity method has been also discussed. The dimension of the sample and the ratio between the surface resistance of the host cavity and the sample are the most important parameters to determine the limit of the measurement.

Finally a cylindrical silver cavity fully coated with YBCO film has been fabricated by electrophoretical deposition. We measure the quality factors and shifts of the resonant frequencies of the cavity as the function of the temperature in various modes of TE₀₁₁, TE₁₁₁, TE₂₁₁ and TE₃₁₁. The microwave properties at different incident potential are also investigated. An anomalous RF dissipation was observed. An unexpected increase of the surface resistance with the temperature was found at $T < 50$ K.

1.- INTRODUCTION

The present paper is a part of work about the study of high temperature superconductor properties in radiofrequency field developed in the Group V of INFN, Sezione di Genova. It has been mainly developed in the Ph. D course of Bi Zhang during the last three years⁽¹⁾. The work aims to study the mechanism of dissipation in high temperature superconducting materials at radio frequency fields, which is primary important in order to understand and determine the basic superconducting characteristics of the materials since the surface impedance of the materials at radio frequency are tightly related to these superconducting parameters such as the energy gap Δ_0 , the penetration depth of the field λ , the coefficient length ξ_0 and the mean free path l . From the materials application point of view, it is also important to understand the origins of the dissipative behaviours in high Tc superconductors at rf. There has been a large amount of experimental work on the surface impedance of HTc materials (2, 3). Generally, high Tc materials show experimentally a relatively high residual surface resistance at low temperature. It seems that the granular structure related properties of the materials are mostly responsible for it (4). Furthermore, the microwave properties are proved to be strongly materials-dependent. The published experimental data were quite various each other⁽⁵⁾.

To obtain a wide knowledge on the RF properties for the high Tc superconducting materials in this work, a variety of samples including bulk pellets, thick and thin films are studied. The pellets are obtained by the standard solid-state reaction process. The electrophoretical technique is used to deposit the thick films on the silver substrates⁽⁶⁾. While, the epitaxial high quality thin films of YBCO are grown on the dielectric substrates of SrTiO₃ with dimension of 10x10mm by in situ sputtering technique. The micro structure and superconducting properties of the samples are characterised by X-ray diffraction, SEM, standard four-probe method and AC susceptibility, etc..The measurements at radio frequency field are performed by using host-cavity technique which was done by inserting pellets and thin films samples in the cylindrical host cavity of 50mm diameter , 50mm height and operating at mode of TE₀₁₁ at 7.9 GHz. For the disc-shaped thick film samples obtained by electrophoresis we just replace an endplate of the cylindrical cavity with the samples. The sensibility and limit of the measurements are also discussed.

In order to study the microwave properties of the superconducting materials and the mechanism of dissipation in the high frequency fields with maximum sensibility and precision,

a cylindrical silver cavity fully coated by YBCO film has been fabricated by electrophoretical deposition. We measure the quality factors and shifts of the resonant frequencies of the cavity as the function of the temperature in various modes of TE₀₁₁, TE₁₁₁, TE₂₁₁ and TE₃₁₁. The properties in different in-put potential are also investigated.

2. - THE MICROWAVE MEASUREMENT SYSTEM

The microwave characterisations of the materials were carried out in an apparatus with high sensitivity and reproducibility, schematically shown in fig.1. A Leybold Cryogenerator is used to cool the cavity system down to about 20K. The temperature of the cavity system was controlled and monitored by a Lake Shore Temperature Controller. Two Lake Shore calibrated diode thermometers are employed for the temperature measurements. They were attached at the two end plates of the cavity to check the possible temperature gradient throughout the cavity. And it is found that the temperature difference between the upper and lower end plate of the cavity was in the range of 1 K during both cooling down and warming up cycles. The cavity was mounted in a chamber which was maintained in vacuum with a pressure in the order of 10^{-5} mbar by a turbomolecular pump during the measurements.

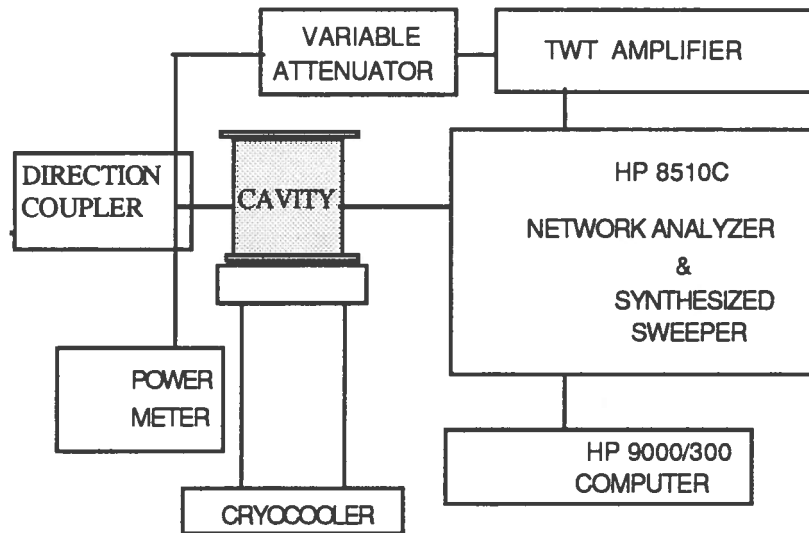


FIG. 1- Schematic diagram of the microwave measurement set-up.

Two magnetic loop antenna were installed in the cylindrical part of the cavity to feed inductively the microwave powers into and extract the transmission signals out of the cavity. To

resolve the degeneration problem of the mode TE011 and TM111 in the cavity, the antenna were lied in the way that the loops of antenna were parallel to the end place of the cavity. To do so, the fluxion lines of magnetic field of mode TE011 transverse through the loop of antenna exciting the mode TE011 in the cavity. While the mode TM111 was not going to be excited because its fluxion lines of magnetic field was not concatenated with the loop of the antenna.

The microwave performances of the system were measured by a HP 8510C Network Analyzer, computer controlled in all measurement processes. The transmission signal S_{21} was used to obtained the quality factors of the cavity based on the following definition of so-called FWHM -3dB method⁽⁷⁾:

$$Q = \frac{f}{\Delta f_{-3dB}}$$

In the case of fully coated cavity with YBCO, the measurements were carried out for different resonant modes of the cavity. In table I the classification and characteristics of the modes were summarised calculated by the code Oscar2D⁽⁸⁾. TE resonant modes were chose in order to minimised the errors due to the losses produced by the current flowing in the cavity joints. Furthermore, in order to study the power dependence of microwave performances of the samples, the output power of the Network Analyzer was fixed at the value of 100 mW. The power level was adjusted by means of a TWT amplifier and a variable attenuator. The RF input power in the cavity was measured with a directional coupler and a bolometric power meter. In this way a wide range of incident power from 0.3 mW to 1 W could be obtained.

TABLE I. Resonant frequencies and geometry factors of the cavity

	TE011	TE11	TE21	TE31
		1	1	1
frequency (GHz)	7.9	4.6	6.5	8.5
geometry factor(Ω)	780	320	370	420

3.- DISCUSSIONS ON THE HOST CAVITY METHOD

A host cavity made by good conducting or superconducting materials ,whose microwave performances are well-known, would be a excellent 'laboratory' to study the microwave properties of the new materials. Following this idea, in fact, the host cavity method has been used in the measurements at RF of high Tc superconducting materials in its early period⁽⁹⁾. The method consists of inserting into or replacing a part of host cavity by the materials to be studied. In our case, we put the small samples of pellets and thin films on SrTiO₃ on the bottom of the host cylindrical silver cavity, and replaced one of end plate of the cavity by a YBCO coated disc silver sample⁽¹⁰⁾.

The principle of the measurements could be briefly given as following. In a general way, the quality factor is related to the surface resistance of the cavity material by:

$$Q = \frac{\Gamma}{R}$$

where Γ describes purely geometrical properties of the cavity depending on the geometrical form of the cavity and the operating mode of the cavity and is defined as:

$$\Gamma = 2\pi f_0 \mu_0 \frac{\int H^2 dV}{\int_S H_{||}^2 dS}$$

When the sample is present inside the cavity, the measurement result can be expressed as

$$\frac{1}{Q} = \frac{R_0}{\Gamma_0} + \frac{R_s}{\Gamma_s}$$

where R_0 and R_s are the silver and the superconducting sample surface resistance, and Γ_0 and Γ_s are the partial geometrical factors defined by the relation:

$$\Gamma_0 = 2\pi f_0 \mu_0 \frac{\int H^2 dV}{\int_{S_0} H_{||}^2 dS_0}$$

$$\Gamma_s = 2 \pi f_0 \mu_0 \frac{\int H^2 dV}{\int_{S_1} H_{//}^2 dS_1}$$

where S_1 is the area of the sample covered surface and S_0 is the rest surface of the host cavity. Therefore, the surface resistance of the materials under study can be expressed as:

$$R_{sc} = \frac{\Gamma_{sc}}{Q} - \frac{(\Gamma_{sc} - \Gamma_{Ag})}{\Gamma_{Ag}} R_{Ag} \quad (1)$$

where Γ_{sc} , Γ_{Ag} is the geometry factors of the superconducting sample and host cavity, R_{Ag} is the surface resistance of the host cavity.

3.1- The Error Limit Of The Measurement

As it has been noted above by eq. (1), the surface resistance of the sample is not to be measured directly. It is related to the measured quality factor Q of the mixed system of the host cavity and sample and the surface resistance of the host cavity as well as the geometry factors of the sample and cavity. Consequently, the error of the measurement is subject to dependent on these parameters. This can be worked out qualitatively by deriving the eq.(1),:

$$dR_{sc} = -\frac{\Gamma_{sc}}{Q} \frac{dQ}{Q} \quad (2)$$

Substituting Q in eq.(1) to this eq. (2), then one can obtained the relative error on the surface resistance of superconducting samples $\frac{\Delta R_{sc}}{R_{sc}}$ is proportional to the that of the quality factor measurement $\frac{\Delta Q}{Q}$ as the following formula:

$$\frac{\Delta R_{sc}}{R_{sc}} = \left(1 + \frac{R_{Ag}}{R_{sc}} \cdot \left(\frac{\Gamma_{sc}}{\Gamma_{Ag}} - 1 \right) \right) \frac{\Delta Q}{Q}$$

It can be seen clearly that the error in the surface resistance of the sample is to be increased linearly not only with the error in the quality factor measurement but also with the ratio of the surface resistance of the host cavity to the superconducting sample and together with that of the geometry factor of the sample to the cavity. Therefore, even though experimentally the error in Q could be controlled at very low level, in the case of small sample with large geometry factor or the host cavity with high resistance, the error in the measurement of surface resistance of the sample would be large.

The fig 2 illustrates the relative error in the surface resistance of the sample as function of the geometry factor of the sample with various ratios of the resistance of the host cavity to that of the sample and the error of quality factor Q is supposed to be 1 percent.

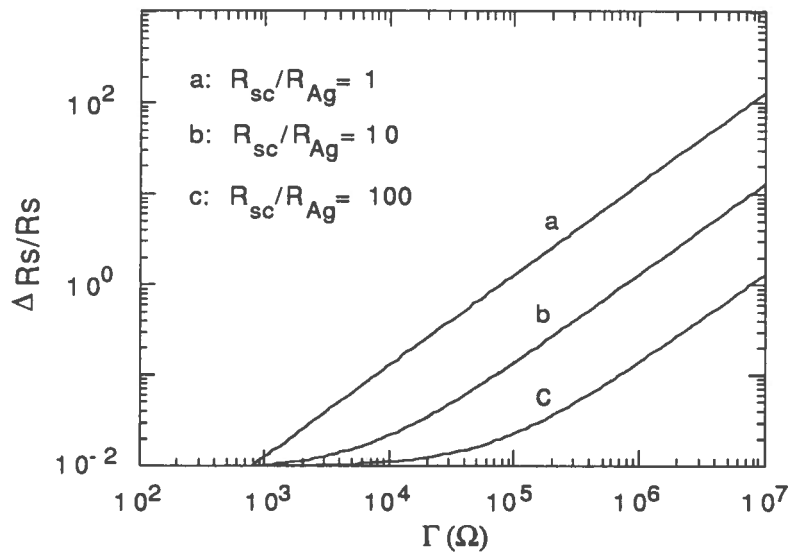


FIG. 2- The relative error of the surface resistance measurement in the host cavity method as a function of the geometry factor of the sample.

4.- SAMPLE PREPARATIONS AND CHARACTERISATIONS

During this work, a number of samples were prepared by using different methods, in order to obtain a wide study about the influence of materials preparing processes on the properties of materials at radio frequency. It's well know that the superconducting properties are

strongly related to material parameters such as the amount of oxygen, the grain orientation and impurities in the materials⁽¹¹⁾, etc.. For example, the superconducting material $\text{YBa}_2\text{Cu}_3\text{O}_x$ changes its superconducting orthorhombic phase to non superconducting tetragonal phase as the content of oxygen x from near 7 to 6. Furthermore, the grain orientations improve the critical current of the superconducting materials. However, how the material processing influence the radio frequency properties of the materials is not quite clear yet.

4.1- Pellet Samples

The bulk materials in form of pellet with dimension 10mm X 2mm were prepared by different solid state reaction processes. The precursor materials of Y_2O_3 , BaCO_3 and CuO were milled and reacted at 900 °C for 10hr; The reacted materials were ground again and pressed into pellets. Then, the pellet called A1 was processed a thermal treatment at 920 °C for 6 hr in fluxion of oxygen. While, the sample A2 was at first calcinated at 940 °C in air for 24 hr, and then followed by the same thermal treatment as sample A1.

The X-ray diffraction analysis shew single orthorhombic superconducting phase structure for both kind of samples. There were no impurities and other phase detected. The temperature dependence of DC resistance of the samples was measured by the standard four-probe method. As shown in fig.3, the pellet A2 shew a very sharp superconducting transition with critic temperature about 92 K and half transition width ΔT about 0.2 K. Meanwhile, the sample A1 gave a wider transition at about 91K with ΔT about 1.5K.

4.2- The Thin Film YBCO on SrTiO_3 Substrate by Sputtering

The YBCO thin films used in this work were deposited on (100) SrTiO_3 single crystal by ion-beam sputtering at the Swiss Federal Institute of Technology ⁽¹²⁾. A detailed description of the preparation of the films is given elsewhere ⁽¹³⁾. The as-deposited films were typically 50-100 nm thick, c-oriented, and shew the following reproducible properties (within the given variations): $T_{\text{CO}}=90\pm 0.5\text{K}$, Transition widths less than 1K, J_c (77K)= $1.0 - 1.2 \times 10^6 \text{ A cm}^{-2}$, ρ (300K) = $300\pm 50 \mu\Omega \text{ cm}^{-1}$, and ρ (300K) / ρ (100K) = 2.9 ± 0.1 .

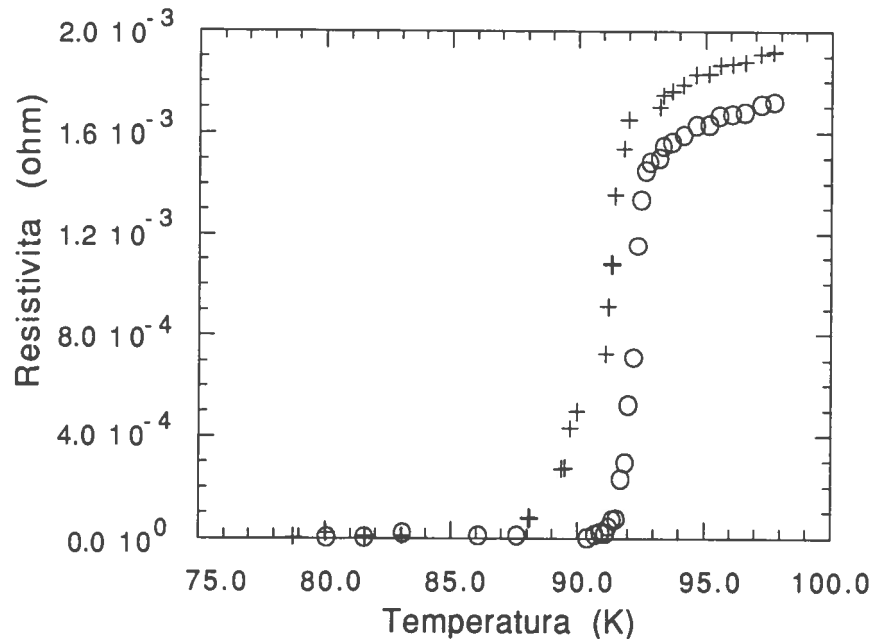


FIG.3- DC resistance of pellets A1 and A2 as function of temperature.

4.3 Thick Films of YBCO by Electrophoretic Deposition

Electrophoresis⁽¹⁴⁾ is a coating technique which enables the deposition of HTCS material on large and curved silver substrates⁽¹⁵⁾ We have developed and used the coating technique of electrophoresis to deposited YBCO superconducting materials on various shape of substrates including a whole cylindrical cavity made of two identical silver disks (55 mm diameter) and a cylindrical body (50 mm inner diameter). In spite of the electrophoretic deposition of many ceramic materials is a well known process, the dynamics of deposition and the charging mechanism of YBCO powders were not well understood yet. In order to develop superconducting cavities a detailed studies on the electrophoretic deposition processes of high Tc materials has been carried out (see appendix I).

The preparation of films using the electrophoretic deposition technique consists of the following three main steps: preparation of suspensions, deposition of films and final thermal treatment. First the suspensions were produced by dispersing the superconducting powders of size about 1 μm in acetone solvent. The fine powder were obtained through mechanical grinding

procedures. The deposition of films consists simply on transferring the suspension to the deposition vessel, inserting the electrodes with the substrate as the cathode, and applying the electrical potential on them. Typical experimental parameters are given in Table II

TABLE II. Typical experimental parameters of electrophoretical deposition

Solvent	Acetone (purity 99.5%)
Substrate	Silver
Temperature	Room Temperature
Suspension Concentration	20-100 g/l
Electrical potential	100-800 V
Electrode distance	10-15 mm
Deposition rate	several $\mu\text{m}/\text{min}$.
Deposition time	~ 1 min

The deposition system for the planar substrates is sketched in fig. 4. In another hand, to coat the cylindrical part of the cavity a copper rod placed along the central axis of the cavity is used as anode while the silver cavity itself is the cathode. The cavity axis is vertical as shown in fig. 5. $\text{YBa}_2\text{Cu}_3\text{O}_{7-x}$ films are deposited on the inner face of the cylindrical cavity by applying a voltage (100 to 400 V) between the electrodes.

By electrophoresis, we succeeded to obtain the as-deposited films showing superconducting transition at about 60 K. However, to improve the superconducting properties of the films, the as-deposited films require appropriate heat treatments. A typical annealing was performed at 920°C for 24 hr. with a short stay at 650°C in oxygen flux. Our $\text{YBa}_2\text{Cu}_3\text{O}_{7-x}$ films deposited on silver substrates had critical temperature at about 90K after heat treatments. A typical value for the critical current density J_c of the sample measured by the standard four-probe DC method was about $500 \text{ A}/\text{cm}^2$ at 77K.

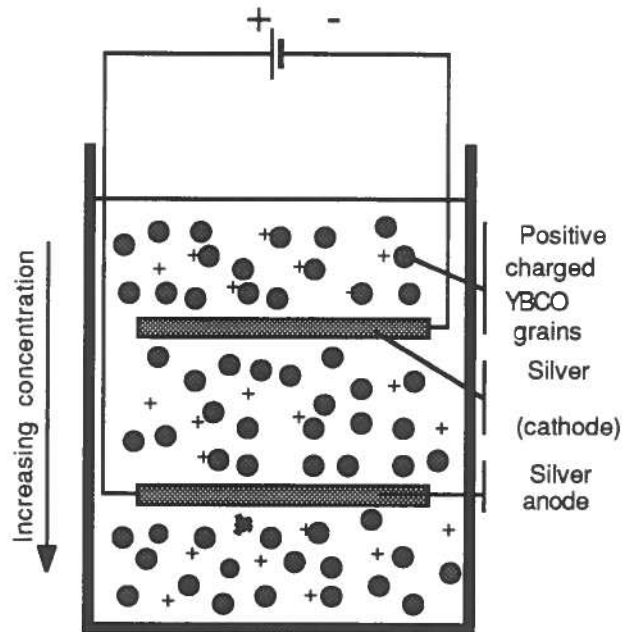


FIG. 4- Schematic view of electrophoretic deposition system for planar substrate.

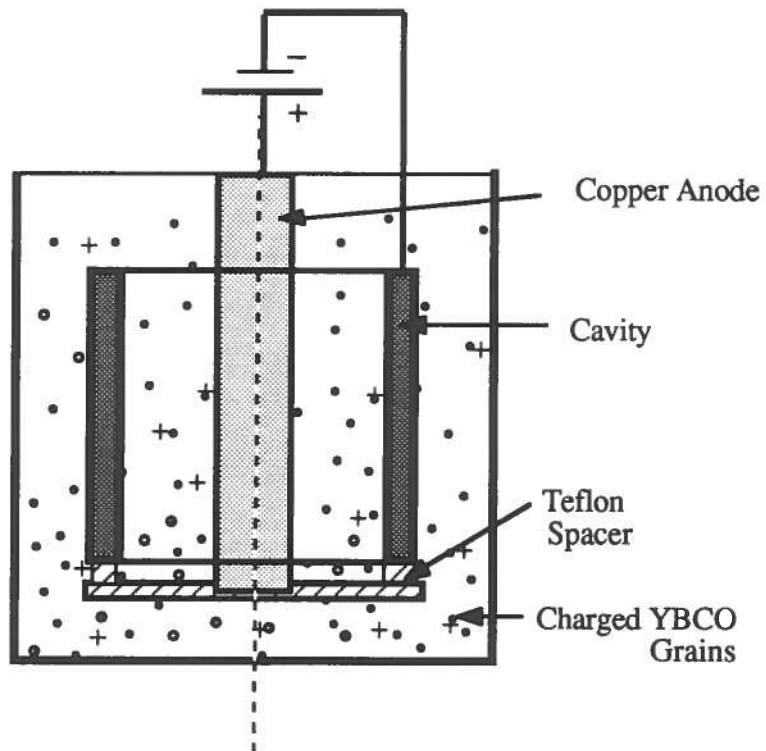


FIG. 5- Schematic representation of electrophoretic deposition system for the cylindrical body of the cavity.

5.- EXPERIMENTAL RESULTS BY HOST CAVITY MEASUREMENTS

By means of the apparatus described in the previous section we measured various kind of samples in the forms of bulk and film. Their preparation is described in the first section and their characteristics are summarised in table III together with their geometry factor Γ in the TE011 mode of the host cavity.

TABLE III. Various samples used in host cavity microwave measurements

	Pellet A1	Pellet A2	Thick film F1	Thick film F2	Thin film
Preparation method	solid state reaction	solid state reaction	electro-deposition	electro-deposition	ion beam sputtering
Dimension	Φ 13 mm	Φ 13 mm	Φ 50 mm	Φ 50 mm	10x10mm
Thickness	3mm	3mm	\sim 30 μ m	\sim 30 μ m	\sim 100nm
T _c (K)	92	92	62	90	90
J _c (77K)A/cm ²				500	10 ⁶
Γ (Ω)	10 ⁵	10 ⁵	10 ⁴	10 ⁴	10 ⁶

The surface resistance of various samples are shown in figures 6, 7, 8 and 9. It was found that the R_s of all samples show a deep decrease at around 90 K with the exception of the electrophoretically deposited film without the heat treatment which have a much lower transition temperature at near 60K. These values were confirmed by dc four-probe and ac susceptibility measurements.

High values of surface resistance for all our samples showing that we have both to improve our sample preparation technique and to increase the sensitivity of our apparatus. The best result we obtained in fact was for the heat treated electrophoretic film on the silver substrate.

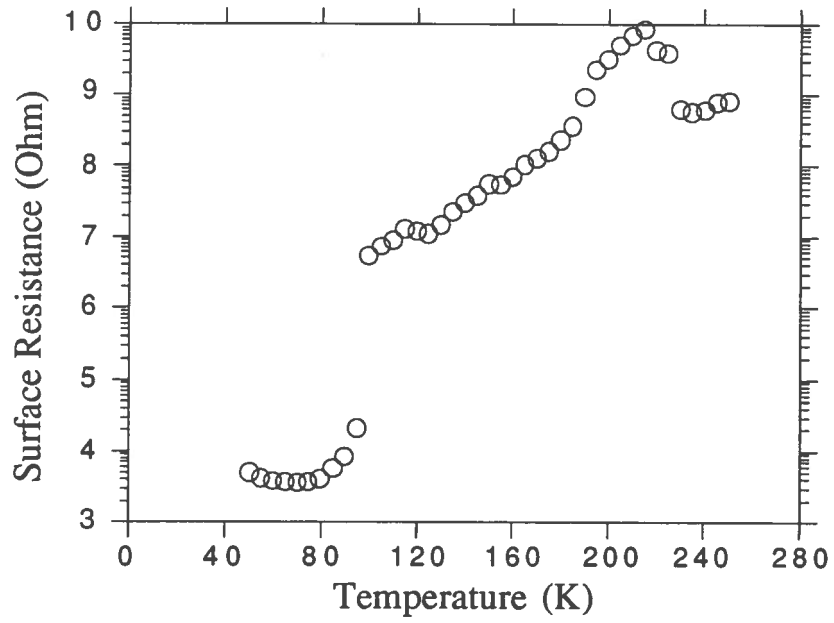


FIG.6- Surface Resistance as function of temperature for the pellet sample A1

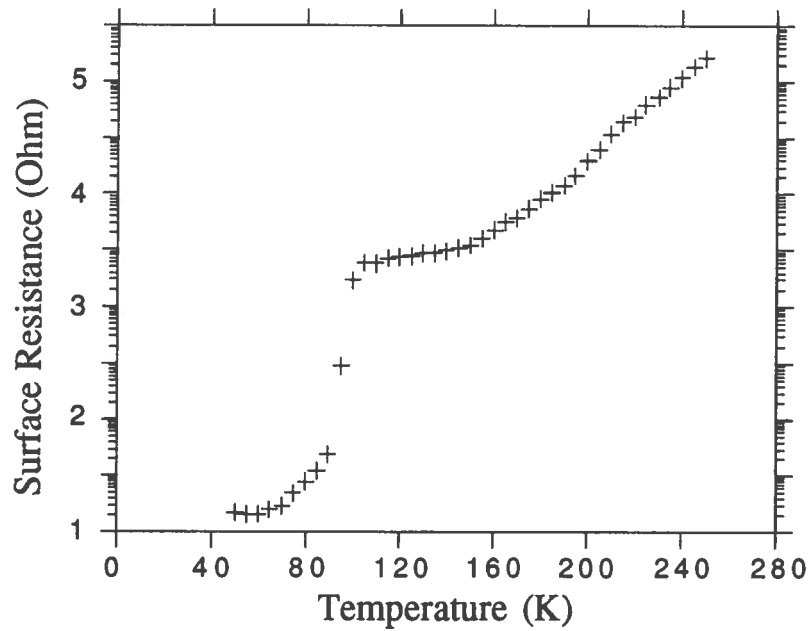


FIG. 7- Surface Resistance as function of temperature for the pellet sample A2

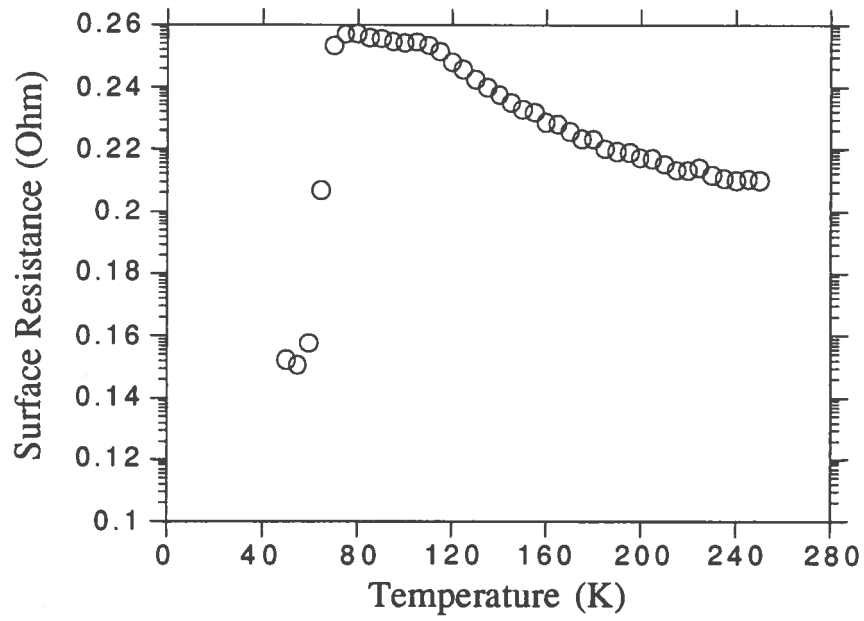


FIG. 8- Surface Resistance as function of temperature for the thick film sample F1

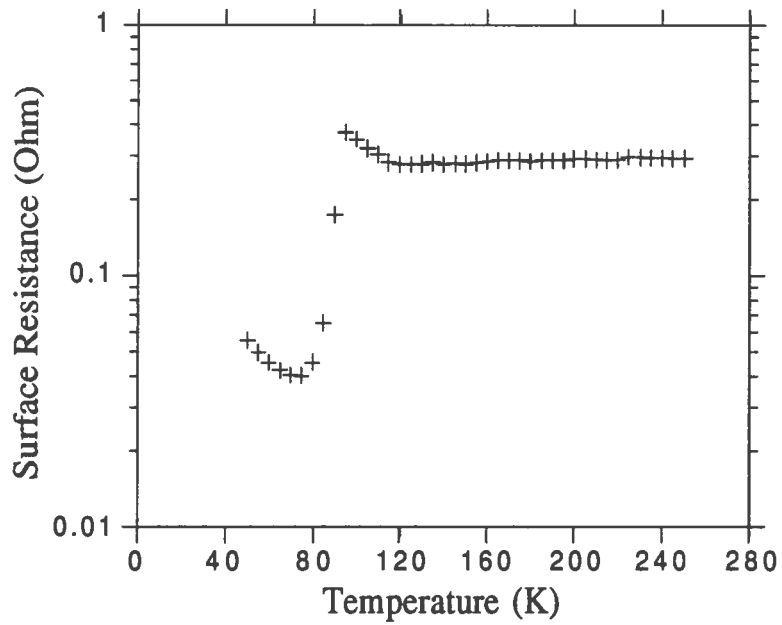


FIG. 9 Surface resistance as function of temperature for the thick film sample F2.

Our results are summarised in table IV. As shown in table IV thick films electrophoretically deposited on silver substrates reached after heat treatment a surface resistance at 50 K of $4 \cdot 10^{-2}$ ohm, of the same order of magnitude of the silver value of $2 \cdot 10^{-2}$ ohm. On the other hand thick films before heat treatment showed at the same temperature a surface resistance of $5 \cdot 10^{-1}$ ohm; this demonstrates the crucial importance of sintering processes in the preparation of electrophoretic films. In our opinion these are good promising results because the preparation method is quite reliable and simple and can be improved looking for the best sintering conditions (temperature level and process time). Furthermore thick films have the best geometric characteristics (lowest geometric factor) between the various samples we studied and so allow easier and more reproducible measurements as discussed in the appendices. In order to obtain geometries more favourable for R.F. measurements we need to deposit an electrophoretic film on the cylindrical cavity surface and to test the R.F. characteristics of this fully covered device.

TABLE IV. Experimental results at RF for various samples

	T _c (K)	R _s (T>T _c)	ρ (T>T _c) mΩcm	δ (T>T _c)	R _s (T=50K)
PELLET A1	92	6.8	139	200	3.8
PELLET A2	92	3.9	46	120	1.1
THICK FILM F1	62	0.26	0.20	8	0.15
THICK FILM F2	90	0.35	0.37	10	0.04

Fig. 10 shows the measured Q of the cavity-sample system obtained for the thin film deposited on dielectric substrates. It is observed strong variations of Q during the measurement when the temperature in the cavity becomes lower than 100 K. Repeated measurements performed on different samples of the same kind taking care to avoid thermal instabilities in the cavity showed the same behaviour. A similar phenomenon, although not as dramatic as ours and in a quite different temperature range, was previously found by other authors ⁽¹⁶⁾. We tried to explain our

result as determined by the anomalous dielectric properties of SrTiO_3 substrate due to the great and strongly temperature dependent dielectric constant and to the high dielectric loss tangent ($\epsilon_r(77\text{K})=1900$, $(d\epsilon_r/dT)=-35 \text{ K}^{-1}$)⁽¹⁷⁾. For these reasons in spite of its good structural properties for YBCO materials, SrTiO_3 has been abandoned as a substrate for high temperature superconductors thin films in favour of more valuable materials for RF applications. The phenomenon we observed can be understood thinking to the sample as a small resonant cavity filled with a dielectric, coupled to the host cavity. Using the OSCAR 2D⁽⁸⁾ and SUPERFISH⁽¹⁸⁾ computer codes we made a numerical calculation of the resonant frequencies of the dielectric cavity at different temperatures and found that for $T \sim 100 \text{ K}$ its fundamental mode coincides with the host cavity operating frequency. When this situation arises a large amount of field is contained in the dielectric, a strong dissipation sets on due to the high dielectric loss and the measured Q drops. Fig. 11 show the system geometry used as input for the numerical calculation, while in fig. 12 the magnetic field lines inside the dielectric are shown. Note that in both figures use is made of the axial symmetry of the system. When the temperature is further lowered the dielectric cavity is no more coupled to the host cavity until higher order modes are excited due to the change in the dielectric constant and the measured Q shows the observed oscillating behaviour. This model gives a qualitative explanation to the observed phenomenon although it cannot explain the details of the $Q(T)$ curve; the minimum at $T \sim 69 \text{ K}$ for example is probably due to the particular field configuration in the dielectric cavity mode excited at that temperature. The result we obtained demonstrates that great care must be taken when a particular dielectric is employed as a substrate for high temperature superconductor devices for RF applications. For this reason we intend to repeat the measurement of thin films grown on more suitable substrates as for example LaAlO_3 in order to obtain results more valuable and comparable to those obtained with other samples.

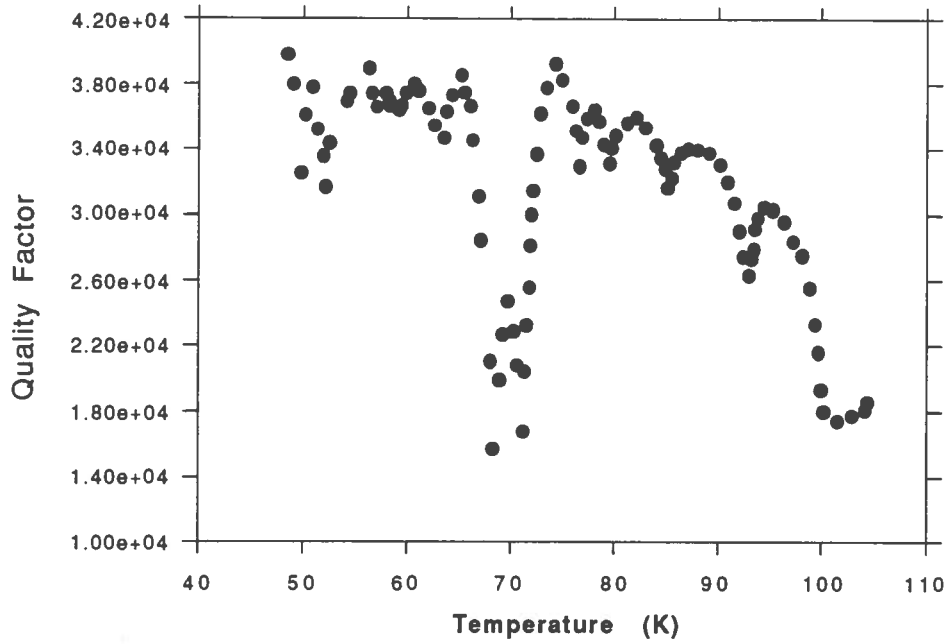


FIG.10- Quality factor in the thin film contained cavity as function of temperature

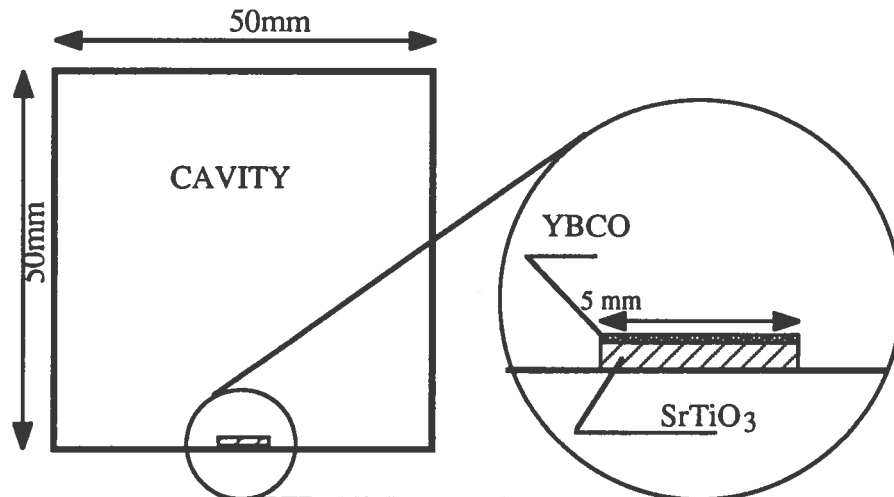
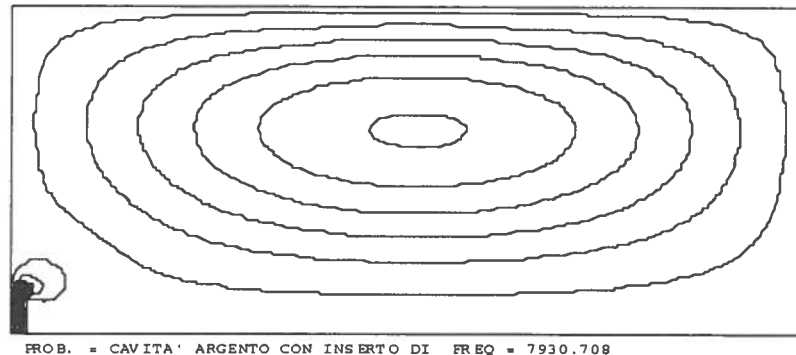
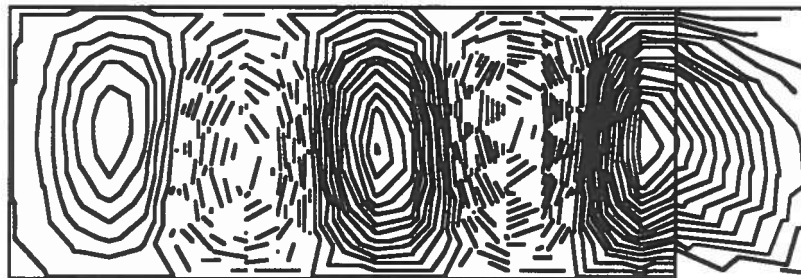


FIG. 11- Schematic geometry of the system composed of host cavity and YBCO thin film on SrTiO₃



(a)



- (b)

FIG. 12- Magnetic field lines plotted by SUPERFISH calculation in the host cavity (a) and inside the dielectric substrate (b).

6. - RESULTS AND DISCUSSIONS ON FULLY YBCO COATED CAVITIES

In order to obtain the most sensible and complete measurement on the microwave performances of the high T_c superconducting materials, as has been pointed before, fully YBCO coated cavities have been fabricated by using electrophoretic deposition technique.

For our first HTSC cavity, a typical measured behaviour of $Q(T)$ and $f(T)$ is shown in fig. 13 for the TE_{011} resonant mode. It is worthwhile noting that in two temperature regions ($T \approx T_c$ and $T \approx 50$ K) a decrease of Q , indicating an increase of power dissipation, is observed, contrarily to what is expected for a standard superconductor. This general behaviour was fully reproducible under repeated cool-down and warm-up cycles; tests made at different RF field levels showed that the curve shape in the region $T \approx T_c$ did not depend on field level while, on the contrary, the

second maximum of R_s that we observed at $T \approx 50$ K, was strongly field dependent (fig. 14). The field dependence of R_s at $T < 50$ K indicates that the dissipation mechanism in this temperature range is determined by the grain coupling rather than by intrinsic grain properties.

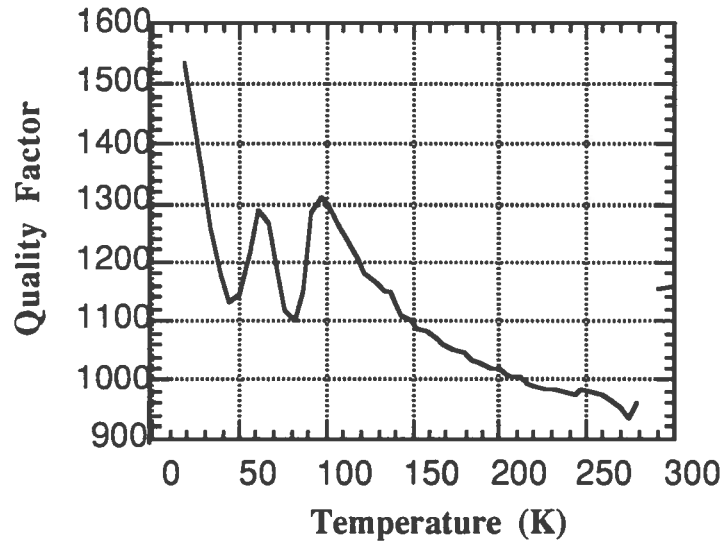


FIG.13- Temperature dependence of the quality factor of the YBCO coated cavity in the TE_{011} mode for an input power of 0.3mW

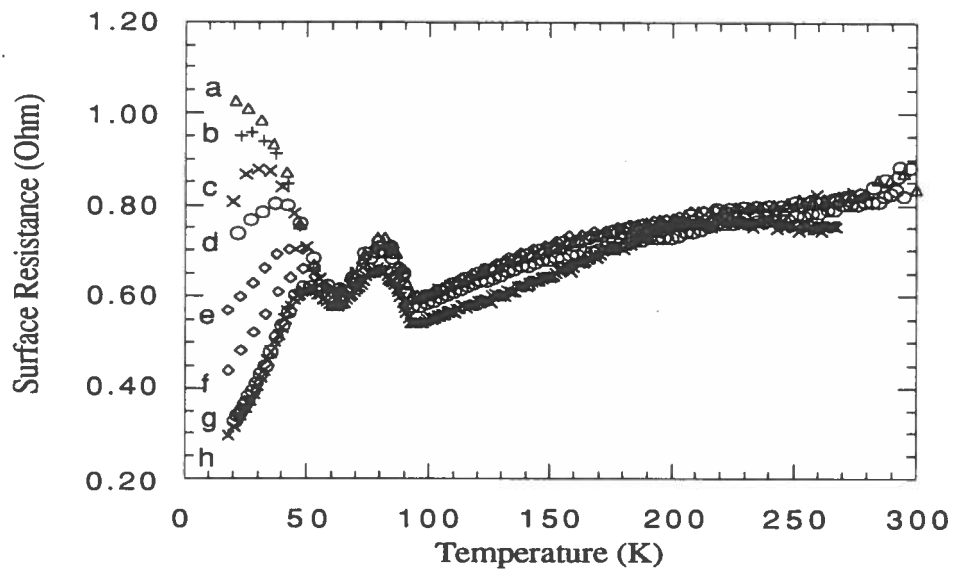


FIG. 14- Temperature dependence of the surface resistance of the YBCO coated cavity in the TE_{011} mode for an input power of (a) 1 W; (b) 600 mW; (c) 270 mW; (d) 100 mW, (e) 50 mW (f) 20 mW, (g) 3 mW and (h) 0.3 mW

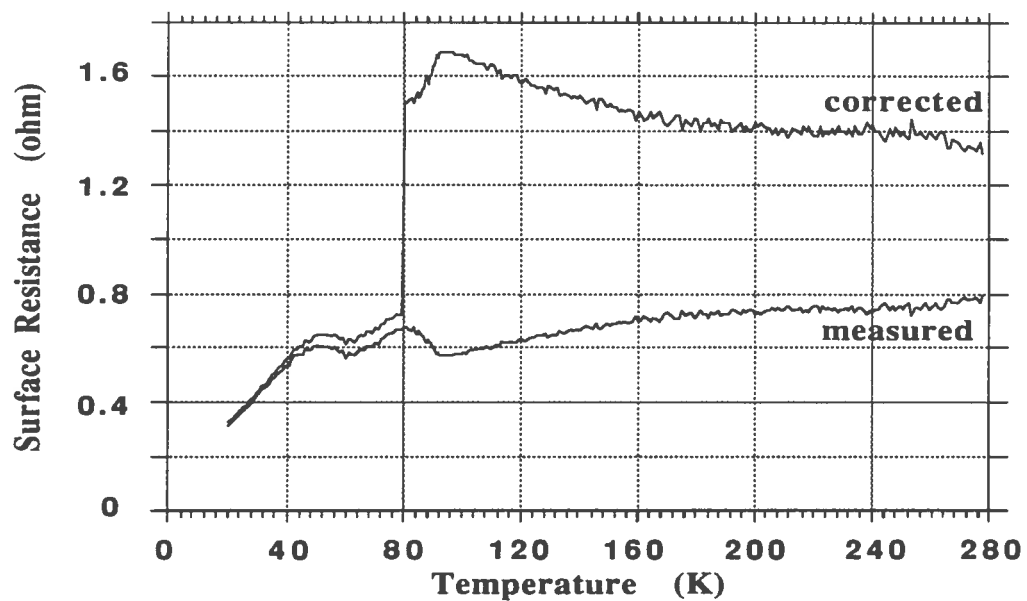


FIG. 15- Comparison between the measured (lower curve) and corrected (upper curve) temperature dependence of the surface resistance of the YBCO coated cavity.

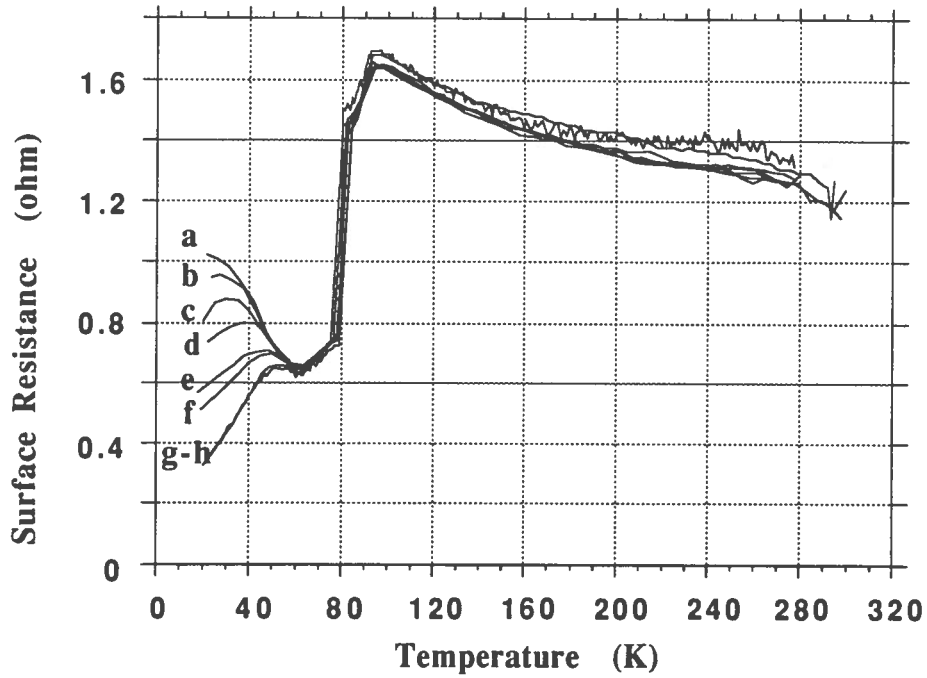


FIG.16- Temperature dependence of the corrected surface resistance of the YBCO coated cavity for different power levels: a) 1 W; b) 600 mW; c) 270 mW; d) 100 mW; e) 50 mW; f) 20 mW; g) 3 mW; h) 0.3 mW;

The behaviour near T_c can be explained taking into account the effect of the silver substrate which plays an important role due to the large field penetration in normal YBCO. In fact we estimated that skin depth in normal YBCO is approximately 50-100 μm , while film thickness is around 30 μm . The solution of the boundary value problem for the surface impedance of the composite system film-substrate yields ⁽¹⁹⁾

$$Z_{meas} = Z_{film} \frac{\sinh(\gamma_{film}d) + \rho \cosh(\gamma_{film}d)}{\cosh(\gamma_{film}d) + \rho \sinh(\gamma_{film}d)} \quad (8)$$

where d is the film thickness, ρ is the ratio between substrate and film surface impedance (i.e. $\rho = Z_{s(subs)}/Z_{s(film)}$) and γ is the propagation constant of the fields inside the film material, defined as for a normal metal:

$$\gamma = (1 + j) \frac{\pi f \mu_0}{R_s} \quad (9)$$

and defined as

$$\gamma = 2\pi f \mu_0 \frac{X_s + jR_s}{X_s^2 + R_s^2} \quad (10)$$

for a superconductor ⁽²⁰⁾ in the framework of a two fluid model, which is generally accepted to hold for ceramic superconductors due to the large value of field penetration depth compared to the short coherence length ⁽²¹⁾. The implicit equation defining Z_{meas} can be solved numerically to find film parameters from measured data once film thickness and substrate surface resistance are known. The result of the calculation, compared to measured R_s values, is shown in figures 15 and 16 where a critical temperature of 85 K was assumed for the film. This is probably a too simplifying assumption since it is conceivable that the superconducting transition develops gradually on the film area with a broad temperature dependence, starting around 90 K and ending at a certain lower temperature. This has been confirmed by magnetic susceptibility measurements performed over a sample of material taken from the cavity coating. Our calculations show that the presence of the substrate let us underestimate by a factor of three the surface resistance of YBCO in the normal state due to the lower surface resistance of silver, while the measurements in the superconducting state are practically unaffected due to the shorter field penetration depth. The corrected data show also a semiconducting-like behaviour of YBCO surface resistance in the normal state which can be a signal of dominant electrical conduction along the c-axis ⁽²²⁾.

However, the anomalous increasing dissipation (under 50 K) as the temperature decrease in the superconducting state is not well understood. The similar behaviour was also observed by some other research groups ⁽²³⁾. Generally, it is related to the behaviour of networks of weakly linked superconducting grains in RF magnetic field.

In fig. 17 the RF surface resistance of the four measured modes is shown. We must point out that only the TE_{0mn} have never transport current in the cavity walls even for perturbed cavity geometries. In TE_{pmn} modes small perturbations induce transport currents across the joints increasing the cavity dissipations ⁽²⁴⁾. Therefore it is difficult to compare data taken in the TE_{011} mode with data taken in the other measured modes and no quantitative statements about the frequency dependence of surface resistance can be made from our data.

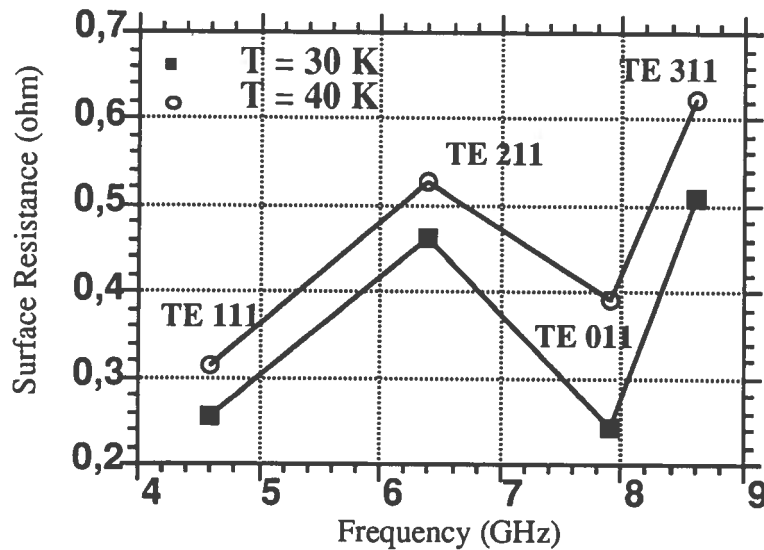


FIG.17- Surface resistance for the four measured modes at 30K and 40 K

In summary, the characterisation of intrinsic properties of high critical temperature superconductors by RF measurements is a difficult task mainly for the high residual resistance values that dominate in a broad temperature range. Furthermore values of material parameters obtained are in fact averages over the whole cavity surface. It is not possible for instance to distinguish between an high level of power dissipation due to a small bad zone (e.g. a defect or an inclusion) on the surface or to the surface material intrinsic properties.

Local imperfections of the film can strongly affect the frequency dependence measurement of material parameters when different resonant modes are used; different fields distribution can in fact enhance dissipations on a point like defect in one mode more than in another. Furthermore one has to take into account dissipations due to current flow in the cavity joints which are different in different modes.

This kind of measurement are greatly affected by inter-grain characteristics, which can be no uniformly distributed over the cavity surface, determining the high residual resistance values reported. Dissipative mechanisms can arise in several ways and various theoretical models have been developed to describe this "weak-link" superconductivity (25).

The obvious advantage of these techniques is that, in view of practical large scale applications of high T_c superconductivity, real devices have to be tested to improve powder preparation technique, film deposition methods and so on. Since neither single crystal

characterisation and grain properties, nor large scale measurements and weak link behaviour give complete information by themselves, both kind of measurements have to be carried on together in a complementary way.

Many problems are still to be solved to obtain high performance for the high T_c superconducting RF cavity. One of the most important subjects is to achieve sufficiently low surface resistance at surface fields as high as a few hundred gauss. We will investigate in the future the influence of microscopic surface structures on RF superconducting properties as well as the frequency dependence of the RF dissipation mechanisms in high T_c films.

APPENDIX I:

Studies On The Electrophoretic Deposition Processes of High T_c Materials

In order to study the electrophoretic deposition process of YBCO powders, two different kind of powders, prepared by standard solid-state reaction method and pyrolytic method, have been used. The pyrolytic powder has finer grains than the solid-state reacted powder, therefore the former powder can be directly suspended in acetone medium without apparent sedimentation, while the latter one needs a previous milling treatment. It has been found that the milling treatment is very important not only for reducing grain size but also for enhancing the electrical charging effect of the grains.

One powder is a commercial product of HiTc Superconco Inc., U.S.A., obtained by standard solid-state reaction method. The grain size of the powder is in the range of 1 μm to several tens of microns, and the fraction of 1 μm grains is about 10 percent. X-ray diffraction result indicates that the powder is very pure and contains only the single orthorhombic phase. The other powder is prepared in our laboratory using pyrolysis of citrates method. The method involves the dissolution of yttrium and copper oxide and barium carbonate with nitric acid. The resulting solution is then combined with citric acid. After evaporation a solid powder material is obtained by pyrolysis. The as-prepared powder has very fine grains (less than 1 micron) with a specific surface area of 4.5 m^2/g , as showed by B.E.T. method. This powder contains different phases such as barium carbonate, yttrium and copper oxides, and the 123 YBCO orthorhombic phase. After a short period sintering treatment at 900°C in air, the as-prepared powder becomes very pure and homogeneous with only the superconducting orthorhombic phase in it. However the sintering procedure produces agglomerates of the fine grains inside the powder, which could not

be used in electrophoretic process. Therefore, we used directly the as-prepared pyrolytic powder in the electrophoretic process instead of the sintered one.

The preparation of suspensions seems to be the most important step. It plays the key role in the whole procedure and determines whether films can be deposited successfully in following deposition step. The suspensions are prepared by dispersing YBCO powders with grain size of about 1 micron into acetone medium. A wet-milling process is used to grind some powders which have large grains and could not be used to form a stable colloidal suspension. In the wet milling process, the YBCO powder is mixed with a small quantity of acetone in a 100 ml grinding bottle. Alumina balls with diameter of 5 mm are used as milling-balls. For the powder prepared by solid-state reaction, it usually needs a long period of milling, typically, more than 24 hours to obtain the right grain size, which is suitable for the formation of a stable suspension for depositing YBCO films. Whereas for the powder prepared by pyrolytic method, normally it only needs about 10 hours milling to get colloidal suspension. Good suspensions can also be prepared without milling due to the fine dimension of grains, but, as shown later, in this case grains are not electrically charged, so no deposition can be obtained.

The film depositions are carried out by applying an electric field between two electrodes, which are placed into the YBCO suspension at about 1 cm distance between each other. The two electrodes are placed vertically in the suspension, and the upper one is the cathode which consists in the silver substrate to be coated. During the deposition process the grains with positive charges migrate upwards the substrate (the cathode) and deposit on it eventually. The sedimentation formed during the procedure does not affect the film coating, due to the vertical arrangement of the electrodes. The applied voltage ranges from 100 V to 800 V. The current density is in the order of $30 \mu\text{A}\cdot\text{cm}^{-2}$ in the beginning of the deposition and usually stays constant in first several minutes, and then it starts to drop down slowly at constant voltage. The decreasing of the current density is due to the depletion of charged grains in the suspension and as a result of the resistance of the YBCO layer deposited on the cathode.

It should be emphasized that the electrical charging process of the grains in the powder is very important for the electrophoretic deposition. It is known that the milling process, apart from reducing the grain size, can also produce surface electrical charges in the grains of the powders. Nevertheless this surface charging effect is not quite clear in the case of high T_c superconductors. In order to study the milling process effect on the deposition rate, various suspensions have been prepared using the two different kind of YBCO powders, prepared by solid-state reaction method and pyrolytic method. Both of two powders have been ground by the milling process for different period of times.

Fig.2 shows the experimental curves of the deposition rates as a function of the milling time for both of the powders. The concentration of the suspensions is 80 g/l and deposit voltage is 200V. The average deposition rate is obtained by measuring the film thickness after 2 minutes deposition.

For the solid-state reacted powder, the amount of deposition is negligible when the milling time is less than 4 hours. After a longer milling treatment an increase in the deposition rate is observed. The deposition rate reaches about 9 $\mu\text{m}/\text{min}$ after 24 hrs milling treatment.

For the pyrolytic powders the deposition rate is about 1 $\mu\text{m}/\text{min}$ after only one hour milling, and then it goes up to about 8 $\mu\text{m}/\text{min}$ when the milling time increases to 8 hours, eventually the deposition rate is saturated at a value of about 11 $\mu\text{m}/\text{min}$ after 24 hours milling. Generally the deposition rate obtained by using pyrolysis powders is higher than that obtained by using the solid-state reacted powders. This result can be explained considering the fact that grains of pyrolytic powders have smaller dimensions than that of solid-state reacted powders. Supposing, for simplicity, the charge per unit area of grain surface is constant, we obtain that the smaller the grains the higher the charge per unit mass. Consequently it results that the small grains in the electric field can move easily upwards to the cathode against the gravitational field. On the other hand, as mentioned before, the pyrolytic powder is fine enough to form a stable colloidal suspension even without previous milling. However, no deposition has been found to take place in such a suspension in the whole voltage range (100-800 V). This phenomenon could be explained in terms of the YBCO grain charging effect during the milling process. It is found that if the powder is not ground before the deposition process, the grains in the suspension will not be sufficiently electrically charged, therefore no movement of grains will take place in the electric field, and consequently no deposition could be obtained. Fig.3 shows the curves of the deposition rate vs the concentration of the suspension for the pyrolytic powder after 20 hours milling in 200V of deposit voltage. It is found from the figure that the deposition rate increases initially with the increasing concentration of suspension, and then it reaches a saturation value in the concentration range of 80 g/l to 100 g/l. However the deposition rate starts to drop down if the concentration of the suspension is further increased to a higher level (more than 100 g/l), because in these highly concentrated suspensions, it is easy to form on the anode a high resistance YBCO layer, due to sedimentation. This high resistance layer shields the electric field in the suspensions.

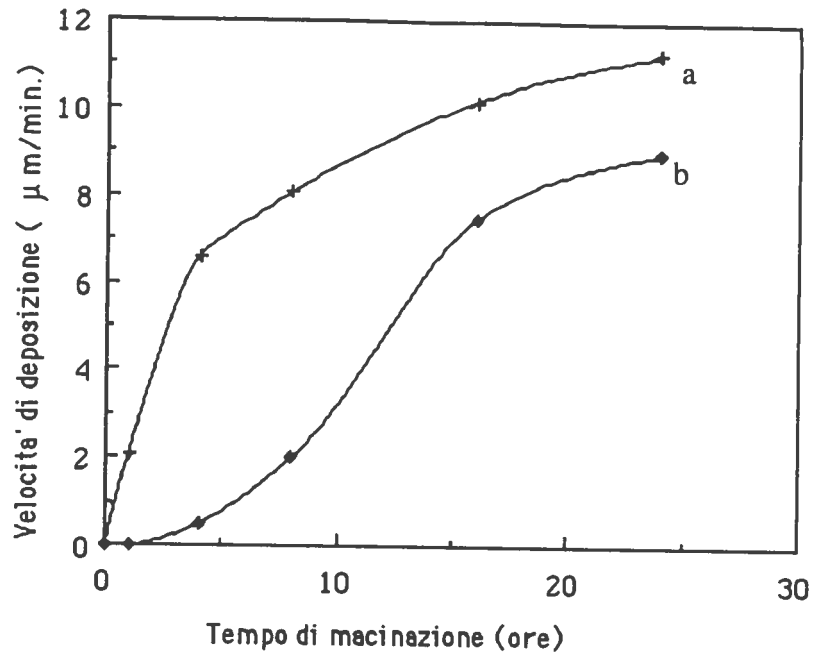


Fig.18 - Deposition rates as function of the milling time for pyrolytic(+) and solid-state reaction (o) powders.

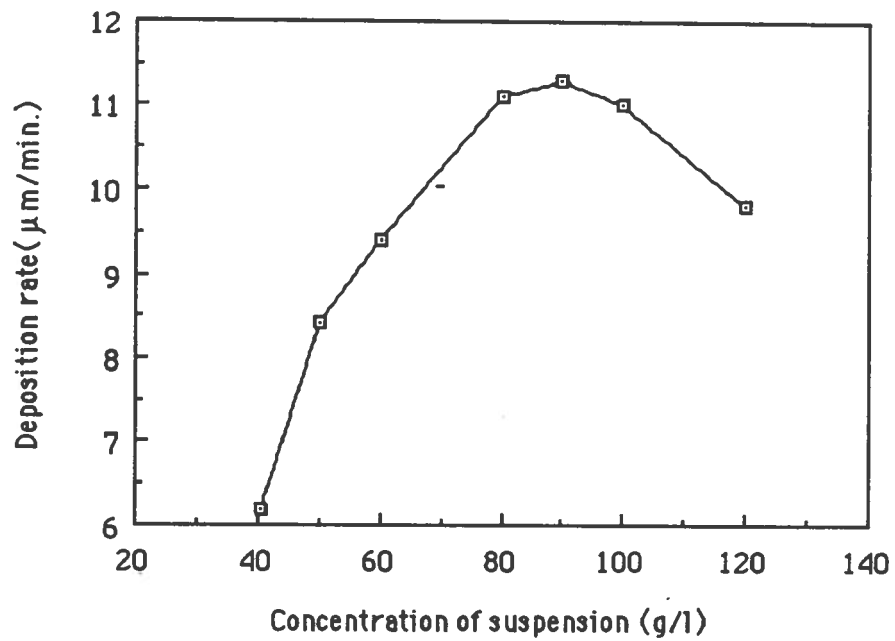


Fig. 19 - Deposition rate vs. concentration of the suspension.

APPENDIX II:

Some Recent Results On The YBCO Cavity at RF Fields

As it has been pointed before, the anomalous dissipation at lower temperature observed in the first YBCO coated cavity at RF is not well understood. There might be several possible causes to be suggested on it, such as the granularity structure of the materials, the impurity inclusions, deficiency of oxygen, quality of CuO chains and more gap behaviour etc.

Recently a modified electrophoretical deposition method has been developed to fabricate an another fully YBCO coated cavity. In this process, the powder was ground without using Al_2O_3 milling balls . To do so, the possible contamination from the corrosion of Al_2O_3 balls in the milling process is to be avoided. Detailed results will be presented in another publication. Here we briefly present some final results on the surface resistance at low rf field and the penetration depth of the field. The anomalous dissipation at low temperature region disappeared. The R_s decreases as the temperature goes down as shown in fig.18. It is clearly seen that the insulate inclusion in the films cause the anomalous dissipation phenomenon in our case. It is interesting to point that the similar aspect in the traditional superconducting films was also observed (26).

Furthermore, the experimental results of the temperature-dependent surface resistance have been best fitted to the BCS theory by using the numeric calculation method (27). The best fit gives a set of characteristic parameters of $YBa_2Cu_3O_7$ films as: $T_c=91K$, $\Delta(0)/kT_c=1.8$, $\lambda_L(0)=6\mu m$, $\xi_0=7\text{\AA}$, and $l=16nm$.

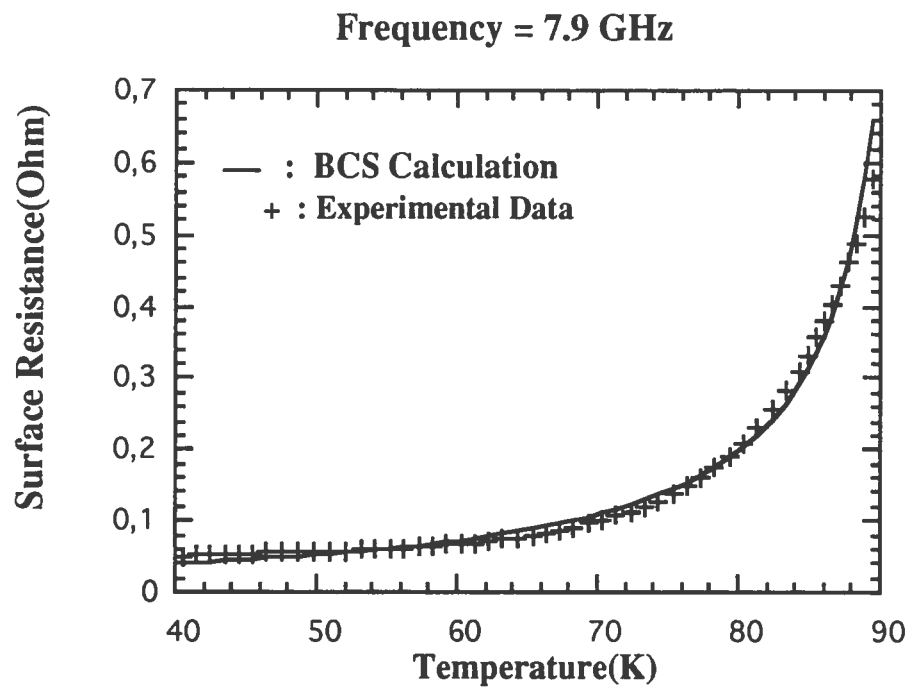


FIG. 20- Surface resistance of the YBCO coated cavity as function of temperature.

REFERENCES:

- (1) B.Zhang, Ph.D. Thesis, Universita' di Genova, 1993
- (2) S.M.Anlage et al., Appl.Phys.Lett., 54, (1989), p.2710
- (3) S.Shridar, C.A.Shiffmen, H.Hamdeh, Phys. Rev.B, 36, (1987), p.2031
- (4) T.L.Hylton et al., Appl. Phys. Lett. 53, (1988), p. 1343; Phys. Rev. B 39, (1989), p.9042.
- (5) G.Mueller, Proceedings of the 4th Workshop on RF Superconductivity, KEK report 89-21, (1990), p.267.
- (6) B.Zhang, P.Fabbricatore, G.Gemme, R.Musenich, R.Parodi, L.Risso, Physica C 193 (1992) 1-7.
- (7) J.D.Jackson Classical electrodynamics, Wiley 1975
- (8) P. Fernandes and R. Parodi, IEEE Trans. Magnet. MAG-21, (1985), p.2246.
- (9) J.R. Delayen, K.C. Goretta, R.B. Poepfel, and K.W.Shepard, Appl. Phys. Lett., 52, 930 (1988).
- (10) P.Fabbricatore, A. Gauzzi, G. Gemme, R.Musenich, R.Parodi, D.Romanengo, B.Zhang, J. Superconductivity, vol. 5, 55-65, 1992.
- (11) R.J. Cava, B. Batlogg, et al. Phys. Rev. Lett., 58, 1676 (1987).
- (12) B.J. Kellett, Appl.Phys.Lett. 57, (1990), p.1146.
- (13) A. Gauzzi, M.L.Lucia, B.J.Kellett, et al. Physica C (1991).
- (14) D.R.Crow, Principles and Applications of Electrochemistry, Chapman and Hall, (1979), London.

- (15) M.Hein, G..Muller, H.Piel, and L.Ponto, *J.Appl.Phys.*, 66 (12), (1989), p.5940.
- (16) N. Klein, G. Mueller, S. Orbach, et al. *Physica C* 162-164, 1549 (1989).
- (17) H. E. Weaver, *J. Phys. Chem. Solids* 11, 274 (1959).
- (18) K. Halbach and R. F. Holsinger, *Particle Accelerators* 7, 213 (1976).
- (19) S.Ramo, J.R.Whinnery, T.Van Duzer, *Field and Waves in Communications Electronics* (Wiley, New York, 1965), p.298
- (20) Y. Kobayashi, T. Imai, H.Kayano, *IEEE Trans. Microwave Theory and Techniques*, MTT-39, (1991), p.1530.
- (21) K.K.Mei, G.Liang, *IEEE Trans.Microwave Theory and Techniques*, MTT-39, (1991) p.1545.
- (22) G.Müller, *Proc. of the 4th workshop on RF superconductivity*, KEK report 89-21, (1990), p.267
- (23) F.J.Rachfort, W.W.Fuller, M.S.Osofsky, *J.Supercond.*, 1, (1989), p.165
- (24) G. Goubau, *Electromagnetic Waveguides and Cavities* (Pergamon, Oxford, 1961) p. 120.
- (25) J. Halbritter, *J. Appl. Phys.* 68 (1990) 6315.
- (26) S. Rubin, T. Schimpfke, et al. *Ann. Physik* 1 (1992) 492-499.
- (27) J. Halbritter, *External report 3/69-2 and 3/70-6 Kernforschungszentrum Karlsruhe*, 1969 and 1970.